polymers

MDPI

Article

Synthesis and Complexation of Well-Defined Labeled Poly(*N*,*N*-dimethylaminoethyl methacrylate)s (PDMAEMA)

Mark Billing [1,2], Tobias Rudolph [1,2], Eric Täuscher [1,3], Rainer Beckert [1] and Felix H. Schacher [1,2,*]

Received: 20 October 2015; Accepted: 23 November 2015; Published: 27 November 2015
Academic Editor: Richard Hoogenboom

[1] Laboratory of Organic and Macromolecular Chemistry, Friedrich Schiller University Jena, Humboldtstr. 10, D-07743 Jena, Germany; mark.billing@uni-jena.de (M.B.); rudolph@dwi.rwth-aachen.de (T.R.); eric.taeuscher@tu-ilmenau.de (E.T.); Rainer.beckert@uni-jena.de (R.B.)
[2] Jena Center for Soft Matter (JCSM), Friedrich Schiller University Jena, Philosophenweg 7, D-07743 Jena, Germany
[3] Laboratory of Chemistry and Biotechnic, Ilmenau University of Technology, Weimarer Str. 25, D-98684 Ilmenau, Germany
* Correspondence: felix.schacher@uni-jena.de; Tel.: +49-3641-948250; Fax: +49-3641-948252

Abstract: We present the synthesis and characterization of well-defined polycationic copolymers containing thiazole dyes in the side chain. Atom transfer radical polymerization (ATRP) was used for the copolymerization of 3-azidopropyl methacrylate (AzPMA) and *N*,*N*-dimethylaminoethyl methacrylate (DMAEMA) of different composition. Thiazole-based alkyne-functionalized dyes (e.g., 5-methyl-4-(prop-2-yn-1-yloxy)-2-(pyridin-2-yl)thiazole, (MPPT)) were afterwards covalently attached using copper catalyzed azide alkyne cycloadditions (CuAAC) reaching contents of up to 9 mol % dye. Subsequent quaternization of the tertiary nitrogen of DMAEMA with strong methylation agents (e.g., methyl iodide) led to permanently charged polyelectrolytes. The materials were characterized by size exclusion chromatography, as well as NMR- and UV/VIS-spectroscopy. Particular attention is paid to the spectroscopic properties of the dyes in the side chain upon environmental changes such as pH and salinity. We anticipate the application of such precisely functionalized polyelectrolytes as temperature- and pH-responsive sensors in biomedical applications, e.g., within interpolyelectrolyte complexes. Concerning the latter, first complex formation results are demonstrated.

Keywords: atom transfer radical polymerization; intense chromophore; micellar interpolyelectrolyte complexes; polyelectrolytes

1. Introduction

Complex and well-defined macromolecular architectures can nowadays be realized by various living and controlled polymerization techniques [1,2]. Owing to increased tolerance of controlled radical polymerizations, a great variety of functional groups can be directly incorporated into materials with narrow molecular weight distributions, predetermined molecular weight, and the possibility of quantitative chain end modification [3,4].

Common techniques are nitroxide mediated polymerization (NMP) [5–7], reversible addition fragmentation chain transfer polymerization (RAFT) [5,8,9], and atom transfer radical polymerization (ATRP) [3,5,10–12]. One clear advantage of ATRP is the availability of a great variety of inexpensive initiators and catalysts, whereas its scope can be limited by side reactions, potentially low yields, and high copper contents in the resulting materials [3]. ATRP is commonly used for differently functionalized acrylates, methacrylates, and styrenic monomers [13–15].

In recent years, many studies focused on poly(*N*,*N*-dimethylaminoethyl methacrylate) (PDMAEMA) as pH- and temperature-responsive material [16–22]. The first ATRP of *N*,*N*-dimethylaminoethyl methacrylate (DMAEMA) was reported by Zhang *et al.* using copper bromide (CuBr) with 1,1,4,7,10,10-hexamethyltriethylenetetramine (HMTETA) and 2,2′-bipyridine (Bpy) as ligands [15,16]. Followed by this, different architectures including star shaped materials were obtained [23,24], and DMAEMA has been used as building block for the preparation of polyampholytes and polyzwitterions [25,26]. Resulting from the pH- and thermo-responsive properties widespread applications such as grafts on films [27] (e.g., polypropylene), the formation of unimolecular micelles [28], or biomedical applications [25] (e.g., shape memory copolymers, or serum-resistant gene delivery and bioimaging) [29] were realized.

As an alternative, post polymerization modification remains a viable tool to incorporate functional groups, which are incompatible even with moderately tolerant controlled radical polymerization (CRP) techniques [3]. Among those, so-called "click" reactions have gained increasing attention due to their high specificity, often quantitative yields, and good tolerance towards other functional groups being present [3]. Since introduction of this term by Fokin, Finn and Sharpless in 2001, "Click chemistry" has been frequently exploited both in applied and fundamental research [30,31]. In that respect, probably the most often used type are copper(I) catalyzed Huisgen-1,3-dipolar cycloadditions between an azide and an alkyne, resulting in 1,4-disubstituted 1,2,3-triazoles [16,32,33]. This reaction could be exploited for the preparation of a variety of different macromolecular architectures [30].

As an example for dye-labeled polycationic polymers, poly(4-vinylbenzyl chloride) was covalently attached to a coumarin dye by Baussard *et al.* [34]. Besides coumarin, additionally aniline-based chromophores were introduced by azo-coupling reactions [35]. Another interesting class of dyes are 1,3-thiazoles. Characterized by their blue emission, high room-temperature fluorescence, large Stokes shifts, and high quantum yields they are a promising class of dyes for a wide field of applications [36–38]. Additionally, the facile introduction of various functional groups and their influence on both absorption and emission enables their application as sensors [36,39,40]. In further studies, it was shown that 4-hydroxy-1,3-thiazoles could be incorporated into various polymeric backbones [9,36,41,42]. This simple synthetic access in combination with enhanced photo-stability also enabled their use in blue emitting polymers [41,43] as well as in light harvesting experiments using Ru(II) polypyridylcomplexes [43,44]. Further, these materials have been employed as sensors for the detection of fluoride [40,45], or as sensitizers in Grätzel-type dye-sensitized solar cells (DSSCs).

Here, we extend the application field of 4-hydroxy-thiazole dyes as side chain chromophores in stimuli-responsive copolymers. Linear copolymers of DMAEMA and AzPMA were synthesized using ATRP and the materials were subsequently labeled using alkyne-functionalized 4-hydroxy-1,3-thiazole dyes via CuAAC. Afterwards, the DMAEMA part of the resulting P(DMAEMA-*co*-AzPMA) copolymers was quaternized and the materials were used as polycations in micellar interpolyelectrolyte complexes (IPECs) [21].

2. Experimental Section

All starting materials were purchased from Sigma-Aldrich (Munich, Germany), Merck (Darmstadt, Germany), or ABCR GmbH (Karlsruhe, Germany) and were used as received if not mentioned otherwise. Tetrahydrofuran, dichloromethane and toluene were purified using a PureSolv-EN™ Solvent purification System (Innovative Technology, Garching, Germany). If necessary, THF and toluene were further dried by refluxing over sodium/benzophenone, while triethylamine (TEA) was distilled over calcium hydride and stored under argon. Any glassware was cleaned in a KOH/*iso*-propanol bath and dried at 110 °C. All deuterated solvents were obtained from Euriso-Top GmbH (Saarbrücken, Germany) and ABCR. The thiazole dye (MPPT) was synthesized according to literature protocols [46]. For dialysis, a Spectra/Por®Dialysis membrane with a molecular weight cut-off (MWCO) of 1000 g·mol^{-1} was used.

2.1. Nuclear Magnetic Resonance Spectroscopy (NMR)

Proton nuclear magnetic resonance (^{1}H NMR) spectra were recorded in $CDCl_3$ (or D_2O, CD_2Cl_2) on a Bruker (Bruker, Karlsruhe, Germany) AC 300-MHz spectrometer at 298 K. Chemical shifts are given in parts per million (ppm, δ scale) relative to the residual signal of the deuterated solvent.

2.2. Size-Exclusion Chromatography (SEC)

2.2.1. Solvent $CHCl_3$

Size exclusion Chromatography was performed on a Shimadzu (Kyoto, Japan) system equipped with a SCL-10A system controller, a LC-10AD pump, and a RID-10A refractive index detector using a solvent mixture containing chloroform ($CHCl_3$), triethylamine (TEA), and *iso*-propanol (*i*-PrOH) (94:4:2) at a flow rate of 1 mL· min^{-1} on a PSS SDV linear M 5-µm column at 40 °C. The system was calibrated with PMMA (410–88,000 g· mol^{-1}) standards.

2.2.2. Solvent DMAc

Size-exclusion chromatography was performed on an Agilent (Santa Clara, CA, USA) system equipped with a G1310A pump, a G1362A refractive index detector, and both a PSS Gram30 and a PSS Gram1000 column in series. *N*,*N*-Dimethylacetamide with 2.1 g· L^{-1} LiCl was applied as eluent at 1 mL· min^{-1} flow rate and the column oven was set to 40 °C. The system was calibrated with PMMA (102–981,000 g· mol^{-1}) standards.

2.2.3. Solvent Water

Size-exclusion chromatography was performed on a Jasco (Groß-Umstadt, Germany) system equipped with a PU-980 pump, a RI-930 refractive index detector, a UV-975 UV/VIS-detector and both a AppliChrom ABOA CatPhil guard 200 Å and an AppliChrom ABOA CatPhil guard 350 Å column in series. Water with 0.1% TFA and 0.1 M NaCl was applied as eluent at 1 mL· min^{-1} flow rate and the column oven was set to 30 °C. The system was calibrated with Dextran (180–277,000 g· mol^{-1}) standards.

2.3. Dynamic Light Scattering (DLS)

DLS measurements were performed using an ALV laser CGS3 Goniometer equipped with a 633 nm HeNe Laser (ALV GmbH, Langen, Germany). DLS measurements were performed at 25 °C and at a detection angle of 90°. The CONTIN analysis of the obtained correlation functions was performed using the ALV 7002 FAST Correlator Software.

2.4. Zeta-Potential Measurements

The ζ-potentials were measured using a Zetasizer Nano ZS from Malvern (Malvern Instruments Ltd, Worcestershire, UK) via M3-PALS technique with a He-Ne laser operating at 633 nm. The detection angle was 13°. The electrophoretic mobilities (u) were converted into ζ-potentials via the Smoluchowski equation:

$$\zeta = \frac{u\eta}{\varepsilon\varepsilon\prime} \quad (1)$$

where η denotes the viscosity and ε the permittivity of the solution.

2.5. Transmission Electron Microscopy (TEM)

TEM measurements were performed on a Zeiss-CEM 902A (Zeiss, Oberkochen, Germany) operated at 80 kV. Images were recorded using a 1 k TVIPS FastScan CCD camera. TEM samples were prepared by applying a drop of an aqueous sample solution onto the surface of a plasma-treated carbon coated copper grid (Quantifoil Micro-Tools GmbH, Jena, Germany).

2.6. UV/VIS Spectroscopy

UV/VIS absorption spectra were recorded with a Specord 250 spectrometer (Analytik Jena, Jena, Germany in Suprasil quartz glass cuvettes 104-QS (Hellma Analytics, Müllheim, Germany) with a thickness of 10 mm. The temperature at the measurements was controlled by a Juno dTRON 08.1 (Analytik Jena).

2.7. Infrared Spectroscopy (IR)

IR spectra were measured on an Affinity-1 ATR FT-IR (Shimadzu, Kyoto, Japan). Dry samples were placed directly on the ATR unit and measured in the range of 600 to 4000 cm^{-1}.

2.8. Synthesis of 3-Azidopropanol

3-Chloropropanol (6 g, 63.47 mmol) was added to a mixture of water (7 mL), sodium azide (8.24 g, 127 mmol), and tetrabutylammonium hydrogen sulfate (0.18 g, 0.53 mmol). The mixture was stirred at 80 °C for 24 h and then at room temperature for 14 h. The product was extracted with diethyl ether three times, the organic phase was dried over sodium sulfate, and the solvent removed under reduced pressure. The final product was obtained as yellow oil in a yield of 76% (4.86 g).

FT-IR: 2100 (azide) cm^{-1}.

^{1}H NMR (300 MHz, $CDCl_3$, δ): 3.66 (t, 2H, –CH_2–OH), 3.37 (t, 2H, –CH_2–N_3), 3.02 (s, 1H, –CH_2–O*H*), 1.76 (tt, 2H, –CH_2–CH_2–CH_2–) ppm.

2.9. Synthesis of 3-Azidopropyl Methacrylate (AzPMA)

A solution of 3-azidopropanol (6 g, 59.3 mmol), triethylamine (7.66 g, 10.5 mL, 75.7 mmol), hydroquinone (150 mg), and methylene chloride (24 mL) was cooled in an ice- bath to 0 °C. Methacryloyl chloride (7.4 g, 6.9 mL, 70.3 mmol) dissolved in methylene chloride (12 mL) was added dropwise over a period of 20 min, and the mixture was stirred for 1 h at 0 °C. Afterwards the solution was allowed to warm to room temperature and stirred for further 14 h. Methylene chloride (25 mL) was added, and the mixture was extracted with an aqueous solution of hydrochloric acid (1/10 *v*/*v*, 2 × 25 mL), water (2 × 25 mL), 10 wt % aqueous NaOH (2 × 25 mL), and again with water. The organic phase was mixed with hydroquinone (0.1 g), dried over sodium sulfate, and the solvent was removed under reduced pressure. The crude oil (10 g) was purified by silica gel column chromatography (methylene chloride) resulting in a colorless oil (6.5 g, 38.6 mmol, 65%, *Caution*: due to its shock sensitive character at higher temperatures special care should be taken).

FT-IR: 2100 (azide) cm^{-1}.

^{1}H NMR (300 MHz, $CDCl_3$, δ): 6.10 (m, 1H, –C=CH_2), 5.57 (m, 1H, –C=CH_2), 4.23 (t, 2H, –CH_2–O–), 3.41 (t, 2H, –CH_2–N_3), 1.91–2.00 (m, 5H, overlapping –CH_2–CH_2–CH_2–, =C–CH_3) ppm.

2.10. General Procedure for the Copolymerization of AzPMA and DMAEMA (P(AzPMA$_x$-co-DMAEMA$_y$))

AzPMA, 1,1,4,7,10,10-hexamethyltriethylenetetramine (HMTETA), *N*,*N*-dimethylaminoethyl methacrylate (DMAEMA), methyl-2-bromoisobutyrate (MEBiB), Cu(I)Br, Cu(II)Br_2 and a small amount of 1,3,5-trioxane, as internal standard, were dissolved in anisole (c_{DMAEMA} = 1.97 mol· L^{-1}). After four freeze-pump-thaw cycles the reaction was stirred at 90 °C for 2 h. Then, the reaction was terminated by the addition of methanol. After removal of copper by an aluminum oxide column (AlOx N), the polymers were further purified via dialysis against THF (Table 1).

[DMAEMA]/[AzPMA]/[CuBr]/[CuBr$_2$]/[HMTETA]/[MEBiB] = [100]/[1;5;10]/[1]/[0.25]/[1]/[1].

^{1}H NMR (300 MHz, $CDCl_3$, P(AzPMA$_{0.09}$-*co*-DMAEMA$_{0.91}$), δ): 4.04 (m, –COO–CH_2), 3.42 (m, –CH_2–N_3), 2.56 (m, CH_2–N(CH_3)$_2$), 2.27 (m, –CH_2–N(CH_3)$_2$), 2.09–1.67 (m –C–CH_2–C–), 0.71–1.17 (m, –C–CH_3) ppm.

Table 1. Size-Exclusion Chromatography (SEC) data of P(AzPMA$_{0.09}$-*co*-DMAEMA$_{0.91}$), P(AzPMA$_{0.05}$-*co*-DMAEMA$_{0.95}$), P(AzPMA$_{0.01}$-*co*-DMAEMA$_{0.99}$).

Sample	M_n [a] (g·mol^{-1})	Đ [a]
P(AzPMA$_{0.09}$-*co*-DMAEMA$_{0.91}$)	13,200	1.14
P(AzPMA$_{0.05}$-*co*-DMAEMA$_{0.95}$)	13,600	1.15
P(AzPMA$_{0.01}$-*co*-DMAEMA$_{0.99}$)	14,600	1.12

[a] SEC ($CHCl_3$/*i*-PrOH/TEA): PMMA-calibration.

2.11. General Procedure for the CuAAC Cycloaddition between P(AzPMA$_x$-co-DMAEMA$_y$) Copolymers and an Alkyne-Functionalized Thiazole-Dye

P(AzPMA$_x$-*co*-DMAEMA$_y$), 5-methyl-4-(prop-2-yn-1-yloxy)-2-(pyridin-2-yl)thiazole (MPPT) and Cu(I)Br were dissolved in THF (30 mL) (Feed ratio: [azide]/[MPPT]/[Cu(I)]/[PMDETA] = [1]/[1]/[0.55]/[0.5]; $c_{copolymer}$ = 2.4 × 10^{-4} mol·L^{-1}). After four freeze-pump-thaw cycles the reaction mixture was stirred at room temperature for 48 h. After removal of copper by an aluminum oxide column the polymers were further purified via dialysis (molecular weight cut off [MWCO]: 1000 g·mol^{-1}). After drying, a slightly yellow solid was obtained.

^{1}H NMR (300 MHz, CD_2Cl_2, P(AzPMA*$_{0.09}$-*co*-DMAEMA$_{0.91}$), δ): 8.50–7.10 (m, Ar*H*, overlapping –N–C*H*=C(CN)), 4.50 (m, –O–CH_2-triaszole ring), 3.98 (m, –COO–CH_2), 3.6 (m, –CH_2-triazole ring), 2.50 (m, CH_2–N(CH_3)$_2$), 2.20 (m, –CH$_2$–N(CH_3)$_2$, overlapping CH_3–C=), 1.98–1.66 (m, –C–CH_2–C–), 0.66–1.03 (m, –C–CH_3) ppm.

2.12. General Procedure for the Quaternization of the Functionalized P(AzPMA$_x$-co-DMAEMA$_y$) Copolymers

Exemplarily, P(AzPMA$_{0.09}$-*co*-DMAEMA$_{0.91}$) and methyl iodide (MeI; 30 fold-excess with respect to the DMAEMA units in the corresponding copolymer) were dissolved in water/dioxane (0.45 mL/0.45 mL; $c_{copolymer}$ = 2.9 × 10^{-3} mol·L^{-1}) and stirred for two days at 38 °C. Afterwards, the excess MeI was removed under reduced pressure. The resulting solution was freeze dried, resulting in a yellow solid.

^{1}H NMR (300 MHz, D_2O, P(AzPMA*$_{0.10}$-*co*-METAI$_{0.90}$), δ): 9.14–7.85 ppm (m, Ar*H*, overlapping –N–C*H*=C(CN)), 5.7 (m, –O–CH_2–triazole ring), 4.55 ppm (m, –COO–CH_2, overlapping –CH_2-triazole ring), 3.91 ppm (m, –CH_2–N(CH$_3$)$_3$, overlapping –COO–CH_2), 3.34 ppm (m, –CH$_2$–N(CH_3)$_3$), 2.22–1.78 ppm (m, –C–CH_2–C–), 1.44–0.71 ppm (m, –C–CH_3).

2.13. Synthesis of Poly(ethylene oxide)-block-Poly(tert-butylacrylate) (PEO$_{118}$-b-PtBA$_{63}$)

For the synthesis of PEO$_{118}$-*b*-P*t*BA$_{63}$, a bromide functionalized PEO macroinitiator (PEO$_{118}$-Br; MI), CuBr, PMDETA and *t*BA were dissolved in anisole ([MI]/[CuBr]/[PMDETA]/[*t*BAA]/[anisole/*t*BA] = [1]/[1]/[1]/[120]/[2]). The polymerization was carried out at 50 °C for 4 days. Then, the reaction was terminated by cooling down in liquid nitrogen. After removal of copper by a silica gel column, the block copolymer was further purified via dialysis against THF. After removal of the solvent under reduced pressure, the polymer was precipitated in hexane and freeze dried. The composition was determined using ^{1}H NMR spectroscopy.

PEO$_{118}$-*b*-P*t*BMA$_{63}$: Đ = 1.05, determined using SEC ($CHCl_3$/*i*-PrOH/TEA): PMMA-calibration).

^{1}H NMR (300 MHz, $CDCl_3$, δ): 4.2 (m, –CH_2–O–), 3.87–3.47 (m, –CH_2–O–), 3.37 (s, –C–CH_3) ppm, 2.31–2.15 (m, –CH$_2$–C*H*(COOC(CH$_3$)$_3$–), 1.95–1.39 (m, –CH_2–CH(COOC(CH_3)$_3$–) ppm.

2.14. Deprotection of PEO$_{118}$-b-PtBA$_{63}$ to PEO$_{118}$-b-PAA$_{63}$

PEO$_{118}$-*b*-P*t*BuAA$_{63}$ (200 mg) was dissolved in dichloromethane (20 mL) and trifluoracetic acid (TFA, 0.93 mL, 20 fold excess with respect to the *t*BA units) was added and stirred at room temperature for two days. After removal of the solvent in vacuum, the crude product was further purified via

dialysis (Spectra/Por®Dialysis Membrane, MWCO: 1000 g· mol^{-1}). After freeze drying, a solid block copolymer could be obtained (109 mg).

^{1}H NMR (300 MHz, $CDCl_3$, δ): 4.19–3.34 (m, –O–CH_2–CH_2–), 2.3–2.0 (m, –CH_2–), 2.20–1.80 ppm (m, –CH_2–CH(COOC$(CH_3)_3$–), 1.79–1.0 (m, –CH_2–CH(COOH)–) ppm.

2.15. Preparation of Micellar Interpolyelectrolyte Complexes (IPEC)

P(AzPMA*$_{0.05}$-*co*-METAI$_{0.95}$) and PEO_{118}-*b*-PAA_{63} were dissolved in buffer solution pH 10 (Merck, borate buffer) with concentrations of c = 1.0 g· L^{-1}. After stirring overnight, the solutions were filtered (Target (Nylon), 5 µm). Different $Z_{-/+}$ values were obtained by mixing the solutions in the required ratios. The prepared interpolyelectrolyte complexes (IPEC)-solutions were mixed in small glass vials (5 mL) and stirred at room temperature for at least 15 h.

Variation of the ionic strength at IPEC $Z_{-/+}$ = 1.0:

The prepared IPEC-solutions were mixed stepwise with a stock solution of sodium chloride at room temperature until the desired molarities were reached. After the addition, the solutions were allowed to stir 24 h at room temperature.

3. Results and Discussion

Herein, we focus on the synthesis of linear, fluorescently labeled polycations and their potential use in the formation of well-defined micellar IPECs. Therefore, P(AzPMA$_x$-*co*-DMAEMA$_y$) copolymers of different composition were synthesized by atom transfer radical polymerization (ATRP) and subsequently labeled using an alkyne-functionalized thiazole dye (Scheme 1). 3-Azidopropyl methacrylate (AzPMA) was prepared as reported by Sumerlin and coworkers starting from 3-chloropropanol but with slightly altered workup conditions (Figures S1 and S2) [3].

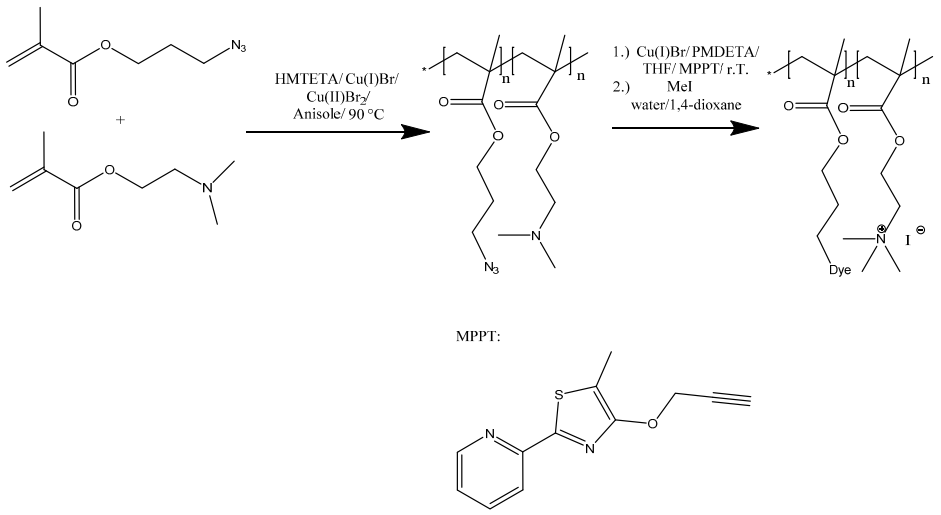

Scheme 1. Copolymerization of DMAEMA and AzPMA, followed by post-polymerization modification via CuAAC between the azide functionalized copolymer and MPPT.

The synthesis of P(AzPMA$_x$-*co*-DMAEMA$_y$) was carried out using Cu(I)Br, Cu(II)Br_2, and 1,1,4,7,10,10-hexamethyltriethylenetetramine (HMTETA) as ligand (Tables 1 and 2). The polymerizations were carried out in anisole at 90 °C ([I]/[Cu(I)/Cu(II)/[HMTETA]/[AzPMA]/[DMAEMA] = [1]/[1]/[0.25]/[1]/[20]/[200]) to approximately 75% conversion (Scheme S1). The reaction progress was monitored by NMR and SEC, thereby confirming the controlled nature of the polymerization (Figure S3).

Via this approach, three different P(AzPMA$_x$-*co*-DMAEMA$_y$) copolymers containing different amounts of AzPMA (1%, 5%, and 9%—Table 2) were synthesized with yields of 26% (P(AzPMA$_{0.09}$-*co*-DMAEMA$_{0.91}$), P(AzPMA$_{0.05}$-*co*-DMAEMA$_{0.95}$)) and 18%

(P(AzPMA$_{0.01}$-*co*-DMAEMA$_{0.99}$)). For all materials, molar masses in the range of 14,000 g·mol^{-1} according to SEC were found. Molecular weight distributions are monomodal and showed narrow dispersity indices (Đ < 1.2, Table S1). After purification via dialysis against THF, no residual monomer could be detected by ^{1}H NMR spectroscopy (Figure S4). FT-IR showed the presence of the azide moiety (Figure S5) for AzPMA contents of 5% and 9%, whereas in case of P(AzPMA$_{0.01}$-*co*- DMAEMA$_{0.99}$) this absorption band is merely visible. The main peaks in ^{1}H NMR at 5.05 (CH_2), 3.41 (CH_2), 2.55 (CH_2), 2.27 (–N(CH_3)$_2$), 1.67–2.08 (–CH_2) and 1.10–0.71 ppm (–CH(CH_3)–) can be attributed to PDMAEMA [47]. The incorporated amount of AzPMA was calculated by comparison of the signals marked as *j* and *h* + *c*, resulting in values of 9%, 5% and 1% incorporated azide functionalities [47,48].

Table 2. Characterization data for P(AzPMA$_x$-*b*-DMAEMA$_y$) copolymers.

Polymers	M_n (g mol^{-1})	Đ	Targeted amount of AzPMA (wt. %)	Incorporated amount of AzPMA [a] (wt. %)	λ_{max1} [d]	λ_{max2} [d]
P(AzPMA$_{0.09}$-*co*-DMAEMA$_{0.91}$)	13,200 [b]	1.14 [b]	10	9	279	-
P(AzPMA$_{0.05}$-*co*-DMAEMA$_{0.95}$)	13,600 [b]	1.15 [b]	5	5	284	-
P(AzPMA$_{0.01}$-*co*-DMAEMA$_{0.99}$)	14,600 [b]	1.12 [b]	1	1	279	-
P(AzPMA*$_{0.09}$-*co*-DMAEMA$_{0.91}$)	11,000 [c]	1.32 [c]	10	9	-	340
P(AzPMA*$_{0.05}$-*co*-DMAEMA$_{0.95}$)	13,700 [c]	1.20 [c]	5	5	-	340
P(AzPMA*$_{0.01}$-*co*-DMAEMA$_{0.99}$)	11,100 [c]	1.18 [c]	1	1	-	334
P(AzPMA*$_{0.09}$-*co*-METAI$_{0.91}$)	5100 [e]	2.02 [e]	10	9	293	351
P(AzPMA*$_{0.05}$-*co*-METAI$_{0.95}$)	7700 [e]	1.67 [e]	5	5	292	358
P(AzPMA*$_{0.01}$-*co*-METAI$_{0.99}$)	11,500 [e]	1.76 [e]	1	1	291	358

[a] Determined via NMR; [b] Determined by SEC ((CHCl$_3$/TEA/*i*-PrOH. (94/2/4)): PMMA-calibration); [c] Determined by SEC ((DMAc/LiCl): PMMA-calibration); [d] Determined using a Specord 250 spectrometer (Analytik Jena) in Suprasil quartz glass cuvettes 104-QS (Hellma Analytics) with a thickness of 10 mm; [e] Determined by SEC ((water, 0.1%TFA, 0.1 M NaCl): Dextran-calibration).

As we intend to use such copolymers as sensors in interpolyelectrolyte complexes, an intense chromophore has to be covalently attached (Figure S6). In that respect, we chose 5-methyl-4-(prop-2-yn-1-yloxy)-2-(pyridin-2-yl)thiazole (MPPT) as model dye. Functionalization with an alkyne moiety enables the use of CuAAC for the covalent attachment to P(AzPMA$_x$-*co*-DMAEMA$_y$) copolymers of different composition.

The copolymers were dissolved in tetrahydrofuran (THF) together with Cu(I)Br, MPPT, and *N*,*N*,*N*′,*N*″,*N*″-pentamethyldiethylenetriamine (PMDETA) and stirred for 48 h at room temperature. After purification via dialysis against THF/water (*v*/*v* 80/20), the labeled copolymers were isolated in good yields of 78% (P(AzPMA*$_{0.09}$-*co*-DMAEMA$_{0.91}$), P(AzPMA*$_{0.05}$-*co*-DMAEMA$_{0.95}$)) and 85% (P(AzPMA*$_{0.01}$-*co*-DMAEMA$_{0.99}$)) by freeze drying and investigated using ^{1}H NMR (Figure S7). Additionally, SEC and UV/VIS measurements were carried out for the modified (P(AzPMA*$_x$-*co*-DMAEMA$_y$)) and non-modified (P(AzPMA$_x$-*co*-DMAEMA$_y$)) copolymers (Figure 1, Table 2).

After attachment of MPPT, the copolymer elution traces from the UV/VIS-detector are a first indication for the success of the reaction. All SEC curves were monomodal and the characteristics of the labeled copolymers are listed in Table 2. The effective degree of functionalization was estimated via NMR (Table 2). Further, the absence of the azide functionality in FT-IR measurements afterwards hints towards complete consumption of AzPMA (Figure S8).

To transform the PDMAEMA part of the copolymers into a strong polycation, quaternization using methyl iodide as strong methylation agent was carried out [49]. Therefore, the respective copolymer P(AzPMA*$_x$-*co*-DMAEMA$_y$) and methyl iodide (30 fold excess) were dissolved in 1,4-dioxane/water (*v*/*v* 1/1) and stirred for 48 h at 38 °C and afterwards P(AzPMA*$_x$-*co*-METAI$_y$) (poly{[2-(methacryloyloxy)ethyl] trimethylammonium iodide}) copolymers with iodide as counter ion could be isolated. SEC in aqueous media confirmed that these copolymers still are UV-active (Figure S9). We attribute the increased Đ in this case to the combination of eluent and column material. According

to NMR, a nearly quantitative quaternization was reached (>98%, Figure 2 and Figure S11) [24]. Due to the different NMR solvents used ($CDCl_3$/CD_2Cl_2) and electronic changes by quaternization, a strong shift of some copolymer signals occurs. For calculation of the quaternization efficiency, the signals marked as *c* and *d* were used (Figure 2) [47].

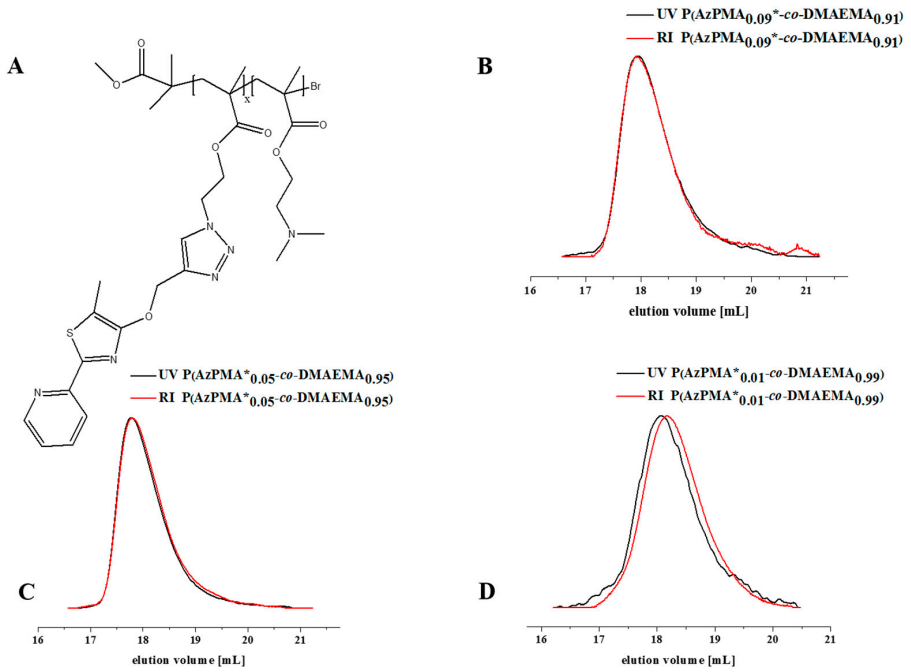

Figure 1. (**A**) Schematic representation of a dye functionalized copolymer; comparison of SEC traces for P(AzPMA*$_x$-*co*-DMAEMA$_y$) (**A**) with different ratios of AzPMA; (**B**) P(AzPMA*$_{0.09}$-*co*-DMAEMA$_{0.91}$), (**C**) P(AzPMA*$_{0.05}$-*co*-DMAEMA$_{0.95}$); (**D**) P(AzPMA*$_{0.01}$-*co*-DMAEMA$_{0.99}$) investigated using RI (black trace) and UV/VIS detector (red trace); eluent: *N*,*N*-Dimethylacetamide with 2.1 g· L^{-1} LiCl, detector wavelength: 360 nm.

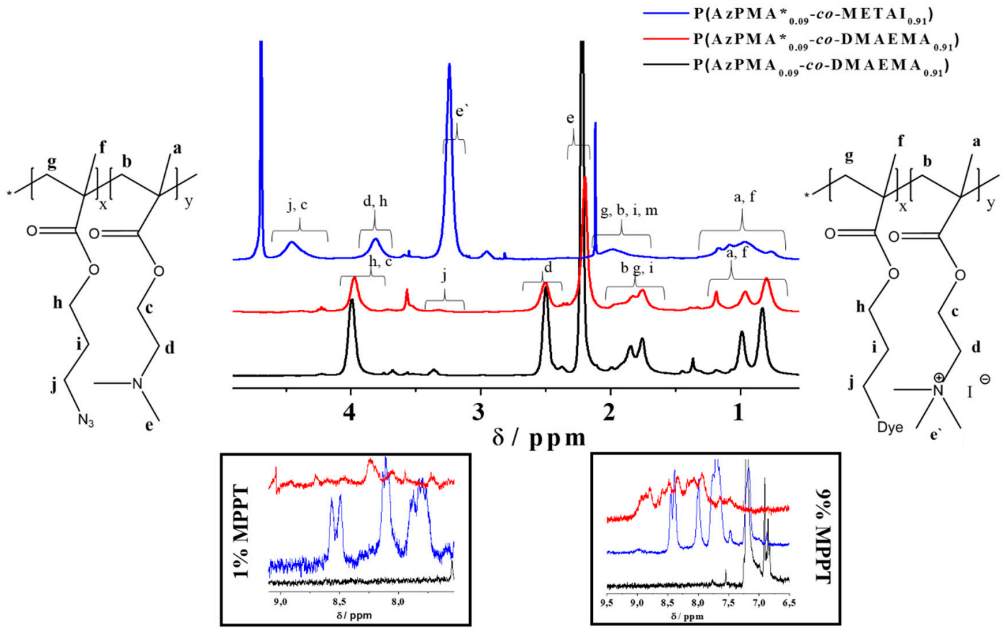

Figure 2. Comparison of ^{1}H NMR spectra for P(AzPMA$_{0.09}$-*co*-DMAEMA$_{0.91}$) (black line, $CDCl_3$), P(AzPMA*$_{0.09}$-*co*-DMAEMA$_{0.91}$) (red line, CD_2Cl_2), P(AzPMA*$_{0.09}$-*co*-METAI$_{0.91}$) (blue line, D_2O); the two insets show the aromatic regions of the copolymers containing 1% and 9% MPPT, respectively.

UV/VIS investigations for all intermediate stages were carried out in water (Figure 3 and Figure S12–S14, Table 2). For all three co-monomer ratios prior to the attachment of the thiazole dye only the absorption of the υ_{azide} 265 nm can be observed (Figure S15). After covalent attachment of the thiazole dye, its characteristic absorption band at 340 nm can be found, even in case of the lowest dye content, P(AzPMA*$_{0.01}$-*co*-DMAEMA$_{0.99}$). Regarding this, no difference between the free and covalently bound dye was observed during our investigations (Figures S6 and S12–S14).

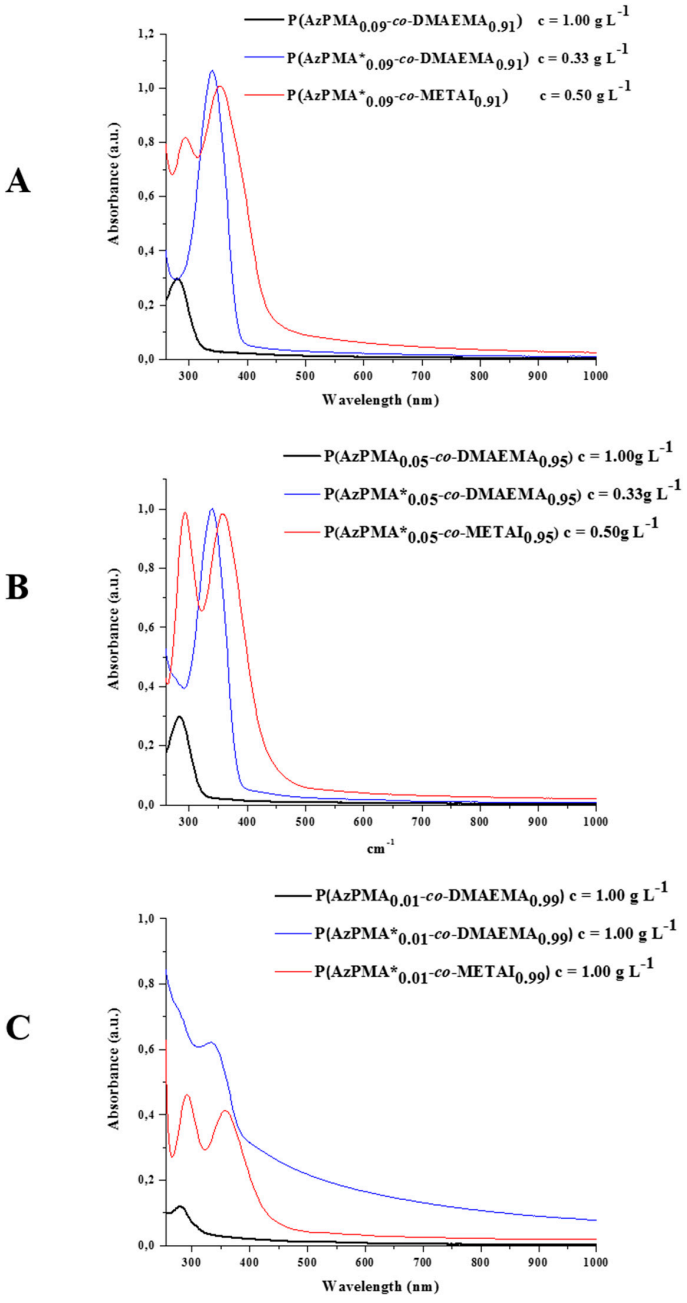

Figure 3. Comparison of UV/VIS spectra for (**A**) P(AzPMA$_{0.09}$-*co*-DMAEMA$_{0.91}$) (black curve), P(AzPMA*$_{0.09}$-*co*-DMAEMA$_{0.91}$) (blue curve) and P(AzPMA*$_{0.09}$-*co*-METAI$_{0.91}$) (red curve); (**B**) P(AzPMA$_{0.05}$-*co*-DMAEMA$_{0.95}$) (black curve), P(AzPMA*$_{0.05}$-*co*-DMAEMA$_{0.95}$) (blue curve) and P(AzPMA*$_{0.05}$-*co*-METAI$_{0.95}$) (red curve); (**C**) P(AzPMA$_{0.01}$-*co*-DMAEMA$_{0.99}$) (black curve), P(AzPMA*$_{0.01}$-*co*-DMAEMA$_{0.99}$) (blue curve) and P(AzPMA*$_{0.01}$-*co*-METAI$_{0.99}$) (red curve, all spectra recorded in water).

After quaternization, the copolymers show different absorption spectra: first, an additional signal at 290 nm can be seen which, according to literature, can be attributed to the presence of I_3^- (absorption maxima at 290 and 360 nm) [50–55]. Second, the absorption band of the dye is shifted to higher λ_{max}. By taking a closer look at the absorption maxima (λ_{max2}), a stronger shift in wavelength with decreasing amount of dye can be observed (9%: $\Delta(\lambda_{max2})$ = 11 nm; 5%: $\Delta(\lambda_{max2})$ = 18 nm; and 1%: $\Delta(\lambda_{max2})$ = 25 nm). This effect might be explained by the interaction of adjacent dye molecules. After methylation, a rather elongated copolymer conformation due to electrostatic repulsion can be anticipated.

To investigate whether MPPT itself is affected by the quaternization reaction, we also subjected the pristine dye to comparable reaction conditions and compared the resulting UV/VIS spectra (Figure 4, Table 3) with those of P(AzPMA*$_{0.09}$-*co*-DMAEMA$_{0.91}$) under both neutral conditions and at pH 10 (the conditions where interpolyelectrolyte complex formation will take place later on). Due to its rather low solubility in aqueous media, UV/VIS spectra of MPPT were measured in THF both before and after quaternization. After quaternization, MPPT displays absorption bands at 299 nm and 349 nm, comparable to the absorption spectra obtained for the labeled copolymers after methylation. Nevertheless, no indication of a successful quaternization of MPPT could be observed by ^{1}H NMR, and therefore we attribute the appearance of a second UV/VIS band to remaining I_3^-. Surprisingly, at pH 10 the first absorption band for the copolymer vanishes and only the absorption at 349 nm can be observed. Further, the absorption band for MPPT broadens and decreases in intensity, which we at this point attribute to the used borate buffer. Further, also the triazole ring will be quaternized under these conditions, but the stability of this moiety after quaternization was previously confirmed by Mishra *et al.* by NMR studies [56].

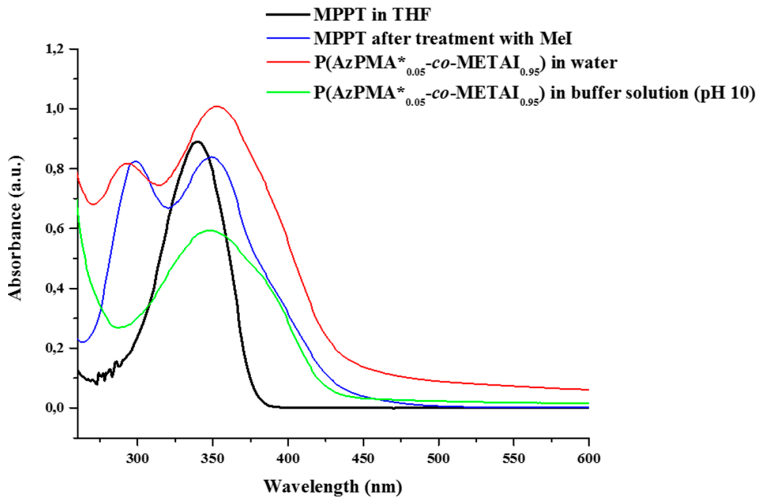

Figure 4. Comparison of UV/VIS spectra of MPPT in THF before (black trace) and, after quaternization (blue trace), P(AzPMA*$_{0.05}$-*co*-METAI$_{0.95}$) in water (red trace) and P(AzPMA*$_{0.05}$-*co*-METAI$_{0.95}$) in buffer solution at pH 10 (green trace).

Table 3. Absorption maxima for the herein used thiazole dye (MPPT) prior and after quaternization as well as P(AzPMA*$_{0.05}$-*co*-DMAEMA$_{0.95}$) under different conditions.

Sample	λ_{max1} (nm)	λ_{max2} (nm)
MPPT [a]	-	340
MPPT after quaternization [a]	299	349
P(AzPMA*$_{0.05}$-*co*-METAI$_{0.95}$) in water	295	351
P(AzPMA*$_{0.05}$-*co*-METAI$_{0.95}$) in buffer solution (pH 10)	-	349

[a] Determined in THF solution using a Specord 250 spectrometer (Analytik Jena) in Suprasil quartz glass cuvettes 104-QS (Hellma Analytics) with a thickness of 10 mm.

Interpolyelectrolyte Complex Formation

In order to use the above described labeled polycations for the formation of micellar interpolyelectrolyte complexes (IPECs) [57], poly(ethylene oxide)-*block*-poly(acrylic acid) (PEO_{118}-*b*-PAA_{63}) was prepared via deprotection of poly(ethylene oxide)-*block*-poly(*tert*-butyl acrylate) (PEO_{118}-*b*-P*t*BuAA_{63}) with trifluoroacetic acid (TFA) at room temperature in dichloromethane (Figure S10). The most prominent ^{1}H NMR signals of PEO_{118}-*b*-P*t*BuAA_{63} in $CDCl_3$ can be observed at 3.34–4.19 ppm (PEO backbone), 2.31–2.15 ppm (PAA backbone) and 1.39–1.95 ppm (*tert*-butyl-group). Successful hydrolysis is indicated by the complete disappearance of the signal for the *tert*-butyl-group. For IPEC formation, P(AzPMA*$_{0.05}$-*co*-MEATI$_{0.95}$) as polycation and PEO_{118}-*b*-PAA_{63} as polyanionic block copolymer were chosen (Scheme 2).

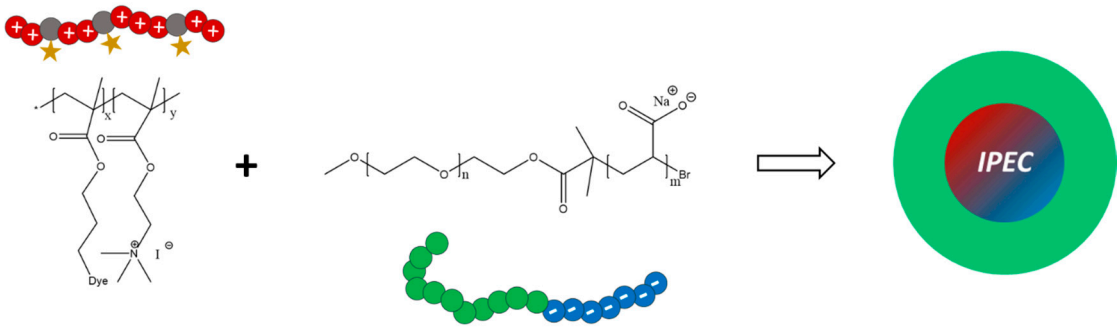

Scheme 2. Schematic representation for the generation of micellar interpolyelectrolyte complexes by mixing P(AzPMA*$_{0.05}$-*co*-MEATI$_{0.95}$) And PEO_{118}-*b*-PAA_{63}.

Using these components a good comparability to previously investigated IPEC systems can be achieved [58]. The *Z*-value represents the mixing ratio according to the used charges and is defined as:

$$Z = \frac{(-)}{(+)} = \frac{overall\ amount\ of\ negative\ charge}{overall\ amount\ of\ positive\ charge} \quad (2)$$

We were interested in whether the dye can be spectroscopically detected after encapsulation within the IPEC core and how this can be influenced by variation of the $Z_{-/+}$-value. For all IPEC solutions only a slight change in turbidity was observed after mixing. All mixtures were prepared in a basic buffer (pH 10) solution, to ensure the complete deprotonation of PEO_{118}-*b*-PAA_{63}.

For IPECs with $Z_{-/+}$-values of 1.5, 1.0 and 0.5 both dynamic light scattering (DLS) and transmission electron microscopy (TEM) measurements were carried out, whereas in (intensity-weighted) DLS experiments, the samples showed the presence of larger aggregates (Figure 5 and Figure S16, Table 4), number-weighted CONTIN plots depicted monomodal size distributions. Here, values of $<R_h>_{n,app}$ = 5 nm ($Z_{-/+}$ = 1.5, Figure 5A), and 10 nm ($Z_{-/+}$ = 0.5, 1.0) are found, respectively. In case of $Z_{-/+}$ = 1.5 most probably mainly block copolymer unimers are detected. Also, TEM measurements for all micellar IPECs confirmed these results as two size distributions were observed, which fit to the values obtained by DLS (Figure 5 and Table 4). In both cases, the IPEC core can be detected and the PEO corona can be ascribed to the grey shadow surrounding the particles. Both single micellar IPECs and clusters thereof are displayed in Figure 5 (and the corresponding insets).

Zeta-potential measurements were further used to evaluate the overall net charge of the formed micellar IPECs and the constituting polyelectrolytes (Table S2), whereas PEO_{118}-*b*-PAA_{63} exhibited −38 mV and P(AzPMA*$_{0.05}$-*co*-METAI$_{0.95}$) +37 mV, the zeta-potentials for the IPECs at all $Z_{-/+}$ ratios were close to charge neutrality. We tentatively explain this finding with the presence of a neutral PEO-shell. The slightly positive value in case of $Z_{-/+}$ = 0.25 can be explained by the excess of polycation.

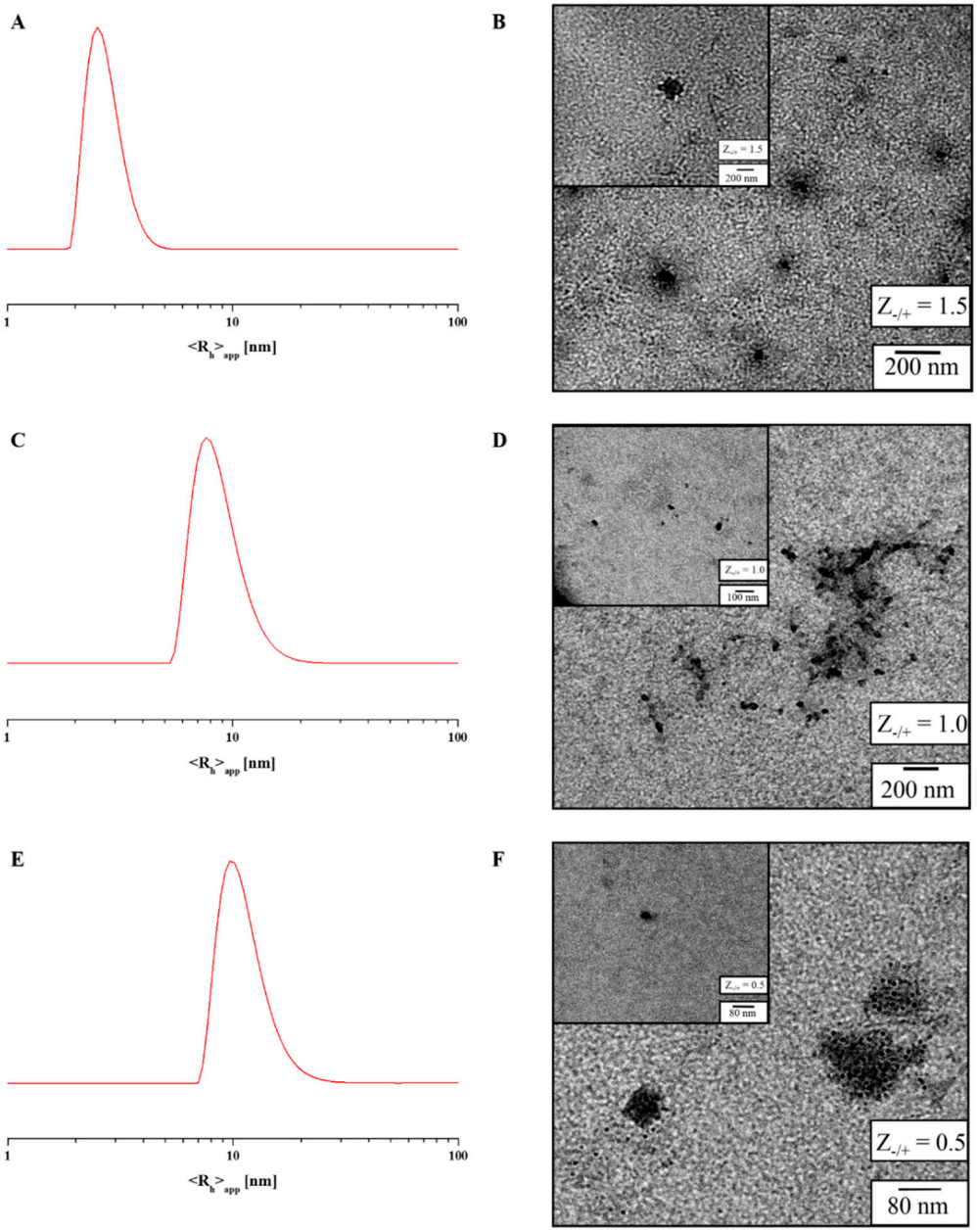

Figure 5. Number-weighted DLS CONTIN plots and TEM micrographs for micellar IPECs formed at $Z_{-/+}$ = 1.5 (**A**,**B**); $Z_{-/+}$ = 1.0 (**C**,**D**); and $Z_{-/+}$ = 0.5 (**E**,**F**).

Table 4. Evaluation of TEM, dynamic light scattering (DLS) and UV/VIS measurements of micellar interpolyelectrolyte complexes (IPECs) in buffer solution at pH 10.

Sample	Diameter (nm) [a]	$\langle R_h \rangle_{n,app}$ (nm) [b]	λ_{max} (nm)	Int.
P(AzPMA*$_{0.05}$-*co*-METAI$_{0.95}$)	-	-	349	0.59
$Z_{-/+}$ = 1.5	80	5	355	0.23
$Z_{-/+}$ = 1.0	56	8	351	0.28
$Z_{-/+}$ = 0.5	35	10	352	0.35
PDMAEMA	-	-	305	0.09

[a] determined via TEM by counting 50 individual IPECs; [b] determined by DLS.

We further investigated the formed micellar IPECs by UV/VIS spectroscopy and compared the results with the previously investigated polycationic copolymers. As can be seen, complex formation seems to induce a slight shift to higher wavelengths for the absorption maxima, depending on charge stoichiometry (Figure S17, Table 4**)**.

Variation of the ionic strength of the surrounding solution is expected to lead to different degrees of swelling of the IPEC core. Starting from nearly salt-free solutions, salinity was increased in steps of 0.2 M by the addition of NaCl up to a final concentration of 1.0 M (Figure S18). Between the addition of salt, the samples were stirred for 24 h. Initially, DLS reveals particle sizes of 20 nm in diameter (Table S3). After the first increase in ionic strength to 0.2 M, a clear decrease in particle size to 3 nm could be observed. This indicates that already this ionic strength is sufficient to dissolve the micellar IPECs, at least partially, increasing the amount of free unimers in solution. Upon further increase of the salt concentration, no significant change was detected. During the experiment, a decrease in UV/VIS intensity was observed as well. Evaluation of the absorption maxima shows a shift to higher wavelengths from 353 to 363 nm during the addition of salt (Table S3).

4. Conclusions

We presented the synthesis and characterization of P(AzPMA*$_y$-*co*-METAI$_x$) copolymers of different composition using ATRP of AzPMA/DMAEMA mixtures, followed by covalent attachment of a thiazole-based dye (MPPT) via CuAAC chemistry and quaternization. Hereby, dye contents of up to 9% could be reached and the labeled copolymers were investigated using a combination of NMR and UV/VIS spectroscopy.

In first experiments, P(AzPMA*$_{0.05}$-*co*-METAI$_{0.95}$) was used for the formation of micellar interpolyelectrolyte complexes with oppositely charged PEO$_{118}$-*b*-PAA$_{63}$ block copolymers, resulting in structures with an IPEC core and a PEO corona. Upon complex formation, a slight shift in UV/VIS absorption of MPPT was detected and micellar IPECs of approximately 20 nm in diameter were formed as shown by a combination of DLS and TEM experiments. We could also demonstrate that increasing the ionic strength of the surrounding medium leads to a further shift of λ_{max} and, apparently, already at 0.2 M NaCl, the IPEC core is re-dissolved. We thus anticipate that such labeled polycationic copolymers can be interesting candidates for monitoring swelling kinetics and solubility changes within IPEC materials, either within solution-borne aggregates or for bulk samples.

Supplementary Materials: Supplementary materials can be found at www.mdpi.com/2073-4360/7/12/1526/s1.

Acknowledgments: The authors thank Tina I. Löbling for the synthesis of PEO$_{118}$-*b*-P*t*BAA$_{63}$ and Grit Festag for water based SEC measurements and helpful discussions. Further, Felix H. Schacher is grateful to the Thuringian Ministry of Science, Education, and Culture (TMBWK; grants #B515-10065, ChaPoNano and #B514-09051, NanoConSens) and Ulrich S. Schubert for continuous support. We would like to acknowledge the NMR-platform at the Friedrich-Schiller-University Jena for support in NMR spectroscopy.

Author Contributions: Mark Billing, Tobias Rudolph and Felix H. Schacher conceived and designed the experiments. Eric Täuscher und Rainer Beckert planned and conducted the synthesis of MPPT. Mark Billing and Felix H. Schacher wrote the paper. All authors discussed the results and commented on the manuscript.

Conflicts of Interest: The authors declare no conflict of interest.

References

1. Xia, J.; Johnson, T.; Gaynor, S.G.; Matyjaszewski, K.; DeSimone, J. Atom transfer radical polymerization in supercritical carbon dioxide. *Macromolecules* **1999**, *32*, 4802–4805. [CrossRef]
2. Webster, O.W. Living polymerization methods. *Science* **1991**, *251*, 887–893. [CrossRef] [PubMed]
3. Sumerlin, B.S.; Tsarevsky, N.V.; Louche, G.; Lee, R.Y.; Matyjaszewski, K. Highly efficient "click" functionalization of poly(3-azidopropyl methacrylate) prepared by ATRP. *Macromolecules* **2005**, *38*, 7540–7545. [CrossRef]

4. Zeng, F.; Shen, Y.; Zhu, S.; Pelton, R. Synthesis and characterization of comb-branched polyelectrolytes. 1. Preparation of cationic macromonomer of 2-(dimethylamino)ethyl methacrylate by atom transfer radical polymerization. *Macromolecules* **2000**, *33*, 1628–1635. [CrossRef]
5. Mansfeld, U.; Pietsch, C.; Hoogenboom, R.; Becer, C.R.; Schubert, U.S. Clickable initiators, monomers and polymers in controlled radical polymerizations—A prospective combination in polymer science. *Polym. Chem.* **2010**, *1*, 1560–1598. [CrossRef]
6. Hawker, C.J.; Bosman, A.W.; Harth, E. New polymer synthesis by nitroxide mediated living radical polymerizations. *Chem. Rev.* **2001**, *101*, 3661–3688. [CrossRef] [PubMed]
7. Iha, R.K.; Wooley, K.L.; Nyström, A.M.; Burke, D.J.; Kade, M.J.; Hawker, C.J. Applications of orthogonal "click" chemistries in the synthesis of soft functional materials. *Chem. Rev.* **2009**, *109*, 5620–5686. [CrossRef] [PubMed]
8. Moad, G.; Rizzardo, E.; Thang, S.H. Living radical polymerization by the RAFT process—A first update. *Aust. J. Chem.* **2006**, *59*, 669–692. [CrossRef]
9. Moad, G.; Rizzardo, E.; Thang, S.H. Living radical polymerization by the RAFT process—A second update. *Aust. J. Chem.* **2009**, *62*, 1402–1472. [CrossRef]
10. Ouchi, M.; Terashima, T.; Sawamoto, M. Transition metal-catalyzed living radical polymerization: Toward perfection in catalysis and precision polymer synthesis. *Chem. Rev.* **2009**, *109*, 4963–5050. [CrossRef] [PubMed]
11. Matyjaszewski, K.; Xia, J. Atom transfer radical polymerization. *Chem. Rev.* **2001**, *101*, 2921–2990. [CrossRef] [PubMed]
12. Kamigaito, M.; Ando, T.; Sawamoto, M. Metal-catalyzed living radical polymerization. *Chem. Rev.* **2001**, *101*, 3689–3746. [CrossRef] [PubMed]
13. Shen, Y.; Zhu, S.; Zeng, F.; Pelton, R. Versatile initiators for macromonomer syntheses of acrylates, methacrylates, and styrene by atom transfer radical polymerization. *Macromolecules* **2000**, *33*, 5399–5404. [CrossRef]
14. Beers, K.L.; Boo, S.; Gaynor, S.G.; Matyjaszewski, K. Atom transfer radical polymerization of 2-hydroxyethyl methacrylate. *Macromolecules* **1999**, *32*, 5772–5776. [CrossRef]
15. Zhang, X.; Xia, J.; Matyjaszewski, K. Controlled/"living" radical polymerization of 2-(dimethylamino)ethyl methacrylate. *Macromolecules* **1998**, *31*, 5167–5169. [CrossRef] [PubMed]
16. Mespouille, L.; Vachaudez, M.; Suriano, F.; Gerbaux, P.; van Camp, W.; Coulembier, O.; Degée, P.; Flammang, R.; Prez, F.D.; Dubois, P. Controlled synthesis of amphiphilic block copolymers based on polyester and poly(amino methacrylate): Comprehensive study of reaction mechanisms. *React. Funct. Polym.* **2008**, *68*, 990–1003. [CrossRef]
17. Ercan, M.T.; Tuncel, S.A.; Caner, B.E.; Piskin, E. 99mTc-labelled monodisperse latex particles coated with amino or carboxyl groups for studies of GI function. *J. Microencapsul.* **1993**, *10*, 67–76. [CrossRef] [PubMed]
18. Kim, E.J.; Cho, S.H.; Yuk, S.H. Polymeric microspheres composed of pH/temperature-sensitive polymer complex. *Biomaterials* **2001**, *22*, 2495–2499. [CrossRef]
19. Patrickios, C.S.; Hertler, W.R.; Abbott, N.L.; Hatton, T.A. Diblock, ABC triblock, and random methacrylic polyampholytes: Synthesis by group transfer polymerization and solution behavior. *Macromolecules* **1994**, *27*, 930–937. [CrossRef]
20. Chen, W.-Y.; Alexandridis, P.; Su, C.-K.; Patrickios, C.S.; Hertler, W.R.; Hatton, T.A. Effect of block size and sequence in the micellization of ABC triblock methacrylic polyampholytes. *Macromolecules* **1995**, *28*, 8604–8611. [CrossRef]
21. Zeng, F.; Shen, Y.; Zhu, S.; Pelton, R. Atom transfer radical polymerization of 2-(dimethylamino)ethyl methacrylate in aqueous media. *J. Polym. Sci. Polym. Chem.* **2000**, *38*, 3821–3827. [CrossRef]
22. Cho, S.H.; Jhon, M.S.; Yuk, S.H.; Lee, H.B. Temperature-induced phase transition of poly(*N*,*N*-dimethylaminoethyl methacrylate-*co*-acrylamide. *J. Polym. Sci. Polym. Phys.* **1997**, *35*, 595–598. [CrossRef]
23. Rikkou-Kalourkoti, M.; Kassi, E.; Patrickios, C.S. Synthesis and characterization of rigid functional anionic polyelectrolytes: Block copolymers and star homopolymers. *J. Polym. Sci. Polym. Chem.* **2012**, *50*, 665–674. [CrossRef]

24. Plamper, F.A.; Schmalz, A.; Penott-Chang, E.; Drechsler, M.; Jusufi, A.; Ballauff, M.; Müller, A.H.E. Synthesis and characterization of star-shaped poly(*N*,*N*-dimethylaminoethyl methacrylate) and its quaternized ammonium salts. *Macromolecules* **2007**, *40*, 5689–5697. [CrossRef]
25. Chen, Y.; Mo, F.; Chen, S.; Yang, Y.; Chen, S.; Zhuo, H.; Liu, J. A shape memory copolymer based on 2-(dimethylamino)ethyl methacrylate and methyl allyl polyethenoxy ether for potential biological applications. *RSC Adv.* **2015**, *5*, 44435–44446. [CrossRef]
26. Lowe, A.B.; McCormick, C.L. Synthesis and solution properties of zwitterionic polymers. *Chem. Rev.* **2002**, *102*, 4177–4190. [CrossRef] [PubMed]
27. Burillo, G.; Bucio, E.; Arenas, E.; Lopez, G.P. Temperature and pH-sensitive swelling behavior of binary DMAEMA/4VP grafts on poly(propylene) films. *Macromol. Mater. Eng.* **2007**, *292*, 214–219. [CrossRef]
28. Steinschulte, A.A.; Schulte, B.; Rutten, S.; Eckert, T.; Okuda, J.; Möller, M.; Schneider, S.; Borisov, O.V.; Plamper, F.A. Effects of architecture on the stability of thermosensitive unimolecular micelles. *Phys. Chem. Chem. Phys.* **2014**, *16*, 4917–4932. [CrossRef] [PubMed]
29. Cheng, L.; Li, Y.; Zhai, X.; Xu, B.; Cao, Z.; Liu, W. Polycation-*b*-polyzwitterion copolymer grafted luminescent carbon dots as a multifunctional platform for serum-resistant gene delivery and bioimaging. *ACS Appl. Mater. Int.* **2014**, *6*, 20487–20497. [CrossRef] [PubMed]
30. Espeel, P.; Prez, F.E.D. "Click"-inspired chemistry in macromolecular science: matching recent progress and user expectations. *Macromolecules* **2015**, *48*, 2–14. [CrossRef]
31. Lava, K.; Verbraeken, B.; Hoogenboom, R. Poly(2-oxazoline)s and click chemistry: A versatile toolbox toward multi-functional polymers. *Eur. Polym. J.* **2015**, *65*, 98–111. [CrossRef]
32. Huisgen, R. 1,3-Dipolar cycloadditions. Past and future. *Angew. Chem. Int. Ed.* **1963**, *2*, 565–598. [CrossRef]
33. Rostovtsev, V.V.; Green, L.G.; Fokin, V.V.; Sharpless, K.B. A stepwise huisgen cycloaddition process: Copper(I)-catalyzed regioselective "ligation" of azides and terminal alkynes. *Angew. Chem. Int. Ed.* **2002**, *41*, 2596–2599. [CrossRef]
34. Baussard, J.-F.; Habib-Jiwan, J.-L.; Laschewsky, A. Enhanced forster resonance energy transfer in electrostatically self-assembled multilayer films made from new fluorescently labeled polycations. *Langmuir* **2003**, *19*, 7963–7969. [CrossRef]
35. Cochin, D.; Laschewsky, A. Layer-by-layer self-assembly of hydrophobically modified polyelectrolytes. *Macromol. Chem. Phys.* **1999**, *200*, 609–615. [CrossRef]
36. Breul, A.M.; Pietsch, C.; Menzel, R.; Schäfer, J.; Teichler, A.; Hager, M.D.; Popp, J.; Dietzek, B.; Beckert, R.; Schubert, U.S. Blue emitting side-chain pendant 4-hydroxy-1,3-thiazoles in polystyrene synthesized by RAFT polymerization. *Eur. Polym. J.* **2012**, *48*, 1339–1347. [CrossRef]
37. Grummt, U.-W.; Weiss, D.; Birckner, E.; Beckert, R. Pyridylthiazoles: Highly luminescent heterocyclic compounds. *J. Phys. Chem. A* **2007**, *111*, 1104–1110. [CrossRef] [PubMed]
38. Schäfer, J.; Menzel, R.; Weiß, D.; Dietzek, B.; Beckert, R.; Popp, J. Classification of novel thiazole compounds for sensitizing Ru-polypyridine complexes for artificial light harvesting. *J. Lumin.* **2011**, *131*, 1149–1153. [CrossRef]
39. Stippich, K.; Weiss, D.; Guether, A.; Görls, H.; Beckert, R. Novel luminescence dyes and ligands based on 4-hydroxythiazole. *J. Sulf. Chem.* **2009**, *30*, 109–118. [CrossRef]
40. Menzel, R.; Kupfer, S.; Mede, R.; Görls, H.; González, L.; Beckert, R. Synthesis, properties and quantum chemical evaluation of solvatochromic pyridinium-phenyl-1,3-thiazol-4-olate betaine dyes. *Tetrahedron* **2013**, *69*, 1489–1498. [CrossRef]
41. Menzel, R.; Breul, A.; Pietsch, C.; Schäfer, J.; Friebe, C.; Täuscher, E.; Weiß, D.; Dietzek, B.; Popp, J.; Beckert, R.; *et al*. Blue-emitting polymers based on 4-hydroxythiazoles incorporated in a methacrylate backbone. *Macromol. Chem. Phys.* **2011**, *212*, 840–848. [CrossRef]
42. Chiefari, J.; Chong, Y.K.; Ercole, F.; Krstina, J.; Jeffery, J.; Le, T.P.T.; Mayadunne, R.T.A.; Meijs, G.F.; Moad, C.L.; Moad, G.; *et al*. Living free-radical polymerization by reversible addition-fragmentation chain transfer: the RAFT process. *Macromolecules* **1998**, *31*, 5559–5562. [CrossRef]
43. Menzel, R.; Ogermann, D.; Kupfer, S.; Weiß, D.; Görls, H.; Kleinermanns, K.; González, L.; Beckert, R. 4-Methoxy-1,3-thiazole based on donor-acceptor dyes: Characterization, X-ray structure, DFT calculations and test as sensitizers for DSSC. *Dyes Pigments* **2012**, *94*, 512–524. [CrossRef]

44. Menzel, R.; Täuscher, E.; Weiß, D.; Beckert, R.; Görls, H.Z. The combination of 4-hydroxythiazoles with azaheterocylces: Efficient bidendate ligands for novel ruthenium complexes. *Anorg. Allg. Chem.* **2010**, *636*, 1380–1385. [CrossRef]
45. Calderón-Ortiz, L.K.; Täuscher, E.; Bastos, E.L.; Görls, H.; Weiß, D.; Beckert, R. Hydroxythiazole-based fluorescent probes for fluoride ion detection. *Eur. J. Org. Chem.* **2012**, 2535–2541. [CrossRef]
46. Täuscher, E.; Weiß, D.; Beckert, R.; Görls, H. Synthesis and characterization of new 4-hydroxy-1,3-thiazoles. *Synthesis* **2010**, 1603–1608.
47. Zhang, J.; Zhou, Y.; Zhu, Z.; Ge, Z.; Liu, S. Polyion complex micelles possessing thermoresponsive coronas and their covalent core stabilization via "click" chemistry. *Macromolecules* **2008**, *41*, 1444–1454. [CrossRef]
48. Bertoldo, M.; Zampano, G.; Terra, F.L.; Villari, V.; Castelvetro, V. Amphiphilic amylose-*g*-poly(methyl)acrylate copolymers through "click" onto grafting method. *Biomacromolecules* **2011**, *12*, 388–398. [CrossRef] [PubMed]
49. Baines, F.L.; Billingham, N.C.; Armes, S.P. Synthesis and solution properties of water-soluble hydrophilic-hydrophobic block copolymers. *Macromolecules* **1996**, *29*, 3416–3420. [CrossRef]
50. Pandeeswaran, M.; Elango, K.P. Spectroscopic studies on the interaction of cimetidine drug with biologically significant σ- and π-acceptors. *Spectrochim. Acta Mol. Biomol. Spectr.* **2010**, *75*, 1462–1469. [CrossRef] [PubMed]
51. Zhang, F.S.; Lynden-Bell, R.M. Interactions of triiodide cluster ions with solvents. *Eur. Phys. J. D* **2005**, *34*, 129–132. [CrossRef]
52. Hanisch, A.; Gröschel, A.H.; Förtsch, M.; Drechsler, M.; Jinnai, H.; Ruhland, T.M.; Schacher, F.H.; Müller, A.H.E. Counterion-mediated hierarchical self-assembly of an ABC miktoarm star terpolymer. *ACS Nano* **2013**, *7*, 4030–4041. [CrossRef] [PubMed]
53. He, S.; Wang, B.; Chen, H.; Tang, C.; Feng, Y. Preparation and antimicrobial properties of gemini surfactant-supported triiodide complex system. *ACS Appl. Mater. Int.* **2012**, *4*, 2116–2123. [CrossRef] [PubMed]
54. Ganesh, K.; Elango, K.P. Spectroscopic and spectrofluorimetric studies on the interaction of albendazole and trimethoprim with iodine. *Spectrochim. Acta Mol. Biomol. Spectr.* **2012**, *93*, 185–197. [CrossRef] [PubMed]
55. Li, N.; Shi, L.; Wang, X.; Guo, F.; Yan, C. Experimental study of closed system in the chlorine dioxide-iodide-sulfuric acid reaction by UV-Vis spectrophotometric method. *Int. J. Anal. Chem.* **2011**. [CrossRef] [PubMed]
56. Mishra, V.; Jung, S.-H.; Jeong, H.M.; Lee, H.-I. Thermoresponsive ureido-derivatized polymers: The effect of quaternization on UCST properties. *Polym. Chem.* **2014**, *5*, 2411–2416. [CrossRef]
57. Pergushov, D.V.; Müller, A.H.E.; Schacher, F.H. Micellar interpolyelectrolyte complexes. *Chem. Soc. Rev.* **2012**, *41*, 6888–6901. [CrossRef] [PubMed]
58. Litmanovich, O.E.; Tatarinov, V.S.; Eliseeva, E.A.; Lapina, A.E.; Litmanovich, A.A.; Papisov, I.M. Formation of copper nanoparticles during the reduction of Cu^{2+} ions in solutions and dispersions of polycation-poly(acrylic acid) interpolymer complexes in acidic media. *Polym. Sci. Ser. B* **2014**, *56*, 326–334. [CrossRef]